An improvement of the upper radiative boundary condition

Günther Zängl
Meteorological Institute, University of Munich, Germany
email: guenther@meteo.physik.uni-muenchen.de

1. Introduction

Since mesoscale numerical models resolve vertically propagating gravity waves, they need an upper boundary condition that prevents spurious reflection of these waves. Currently, two different methods are available. The first one is to use a thick damping layer in the upper part of the model domain that gradually dissipates the wave energy, often called a sponge layer. The damping may either be accomplished with enhanced horizontal diffusion (e.g. Klemp and Lilly 1978) or with linear relaxation to a given basic state (e.g. Saito and Ikawa 1991). Alternatively, as is done in the MM5, a radiative upper boundary condition may be used. The main advantage of a radiation condition is its efficiency. While a sponge layer must extend over more than 10 model levels to yield satisfactory results, only one level is needed for a radiation condition.

Each of these methods has its limitations. A diffusive sponge is useful only if the horizontal resolution is not finer than ∼10 km. At higher resolutions, a significant part of the gravity wave spectrum will not be damped properly. A relaxation to a basic state requires knowledge of this basic state. This is straightforward for idealized simulations, but in general, the basic state has to be computed by some horizontal and vertical averaging or to be interpolated from the NWP analysis data with which the mesoscale model is driven. The most severe weakness of the radiative boundary condition is—similar to the diffusive sponge—the limited range of horizontal wavelengths captured by it (see below). In this paper, a way to overcome this limitation with little additional computational costs is presented.

2. The problem

Since the upper radiative boundary condition (i.e. the vertical wind field in the uppermost model level) has to be computed non-locally by means of a Fourier transform, a local subdomain around each grid point is needed. The extension if this subdomain determines the range of horizontal wavelengths captured by the radiation condition. In the MM5 model, a 13×13 grid centered at each grid point is used. Consequently, the maximum horizontal wavelength that is able to radiate upward is 12 times the grid distance when the wavenumber vector is aligned with the grid. In general, the maximum wavelength is larger by a factor of $\frac{1}{\cos\alpha}$ where α is the smallest angle between the wavenumber vector and one of the coordinate axes. This yields a theoretical maximum of $12\sqrt{2}\Delta x(\approx 17\Delta x)$. Longer waves are reflected back in the same way as if a rigid lid was present at the model's top.

It is easy to see that this wavelength range is insufficient for high-resolution simulations. For typical atmospheric parameters, vertical gravity wave propagation is possible up to wavelengths of several hundreds of kilometers, Coriolis effects being of minor importance up to ∼150 km. Thus, at least for grid distances below 10 km, a significant part of the gravity wave spectrum is reflected back. For illustration, a simulation of idealized flow over a quasi-twodimensional mountain is presented in Fig. 1. The mountain shape is defined by

$$h(x) = \frac{h_o}{(1+\frac{x^2}{a^2})^{1.5}}\,, \qquad (1)$$

h_o and a being 300 m and 40 km, respectively. A uniform flow with $U = 10\,\mathrm{m\,s^{-1}}$ and $N = 10^{-2}\,\mathrm{s^{-1}}$ is prescribed, and Coriolis effects are turned off. Evidently, the model fails to reproduce the characteristic upstream phase shift of vertically propagating gravity waves.

3. An efficient solution

The modification presented here makes use of the

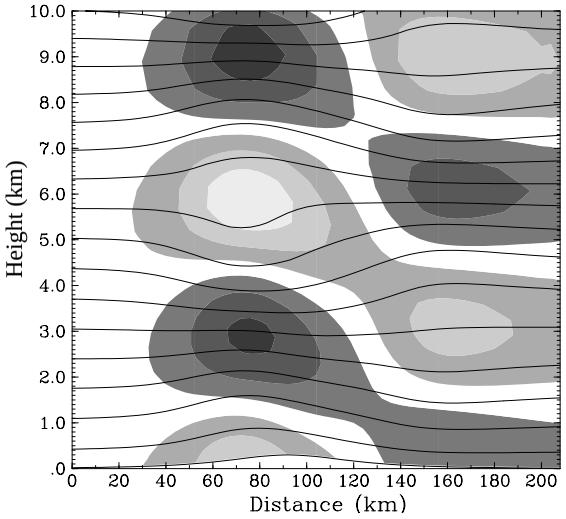

Figure 1: Vertical cross-section along the center of the mountain ridge. Solid lines: Potential temperature, contour interval 2 K; shading: horizontal wind speed, shading steps $2\,\mathrm{m\,s^{-1}}$, no shading between 9 and $11\,\mathrm{m\,s^{-1}}$, dark shading for higher wind speeds, light shading for lower wind speeds. Simulation with original radiation condition.

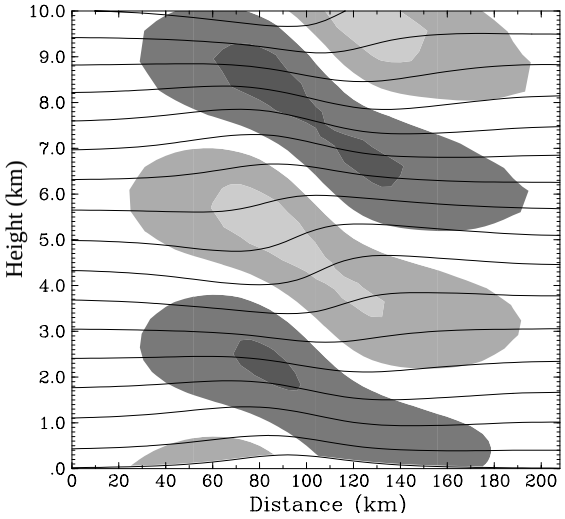

Figure 2: Same as Fig. 1, but for simulation with modified radiation condition.

fact that high-resolution simulations are usually performed on several interactively nested model domains. In this case, wave components too long to be captured by the radiation condition in a nest may be interpolated from the next coarser domain. One just has to ensure that interpolated wave components and wave components computed locally do not overlap because this would yield instability. Thus, the coarse-domain radiation condition must be filtered before being interpolated. This is accomplished with a twodimensional Fourier transform.

Since the nesting ratio is 3 for interactively nested domains, wavelengths $\leq \lambda_o \equiv 4\Delta x$ have to be eliminated if the wavenumber vector $\mathbf{k} = (k_x, k_y)$ is aligned with the grid. In general, the factor $\frac{1}{\cos\alpha}$ mentioned above must be taken into account. For $\lambda_x \leq \lambda_y$ ($\lambda_y \leq \lambda_x$), the maximum wavelength captured by the radiation condition increases by a factor of $\sqrt{1+\frac{\lambda_x^2}{\lambda_y^2}}$ ($\sqrt{1+\frac{\lambda_y^2}{\lambda_x^2}}$). In addition, from $k^2 = k_x^2 + k_y^2$ follows $\lambda_x = \frac{\lambda\lambda_y}{\sqrt{\lambda_y^2-\lambda^2}}$, which means that the projection of the wavelength on the grid λ_x (or λ_y) is longer than the real wavelength λ. Setting $\lambda = \lambda_o\sqrt{1+\frac{\lambda_x^2}{\lambda_y^2}}$ ($\lambda = \lambda_o\sqrt{1+\frac{\lambda_y^2}{\lambda_x^2}}$), one finds that all wavelengths up to

$$\lambda_x = \lambda_y\sqrt{\frac{\lambda_y^2}{2\lambda_o^2} - \frac{\lambda_y\sqrt{\lambda_y^2-4\lambda_o^2}}{2\lambda_o^2} - 1}\;;\; \lambda_x \leq \lambda_y \quad (2)$$

and

$$\lambda_y = \lambda_x\sqrt{\frac{\lambda_x^2}{2\lambda_o^2} - \frac{\lambda_x\sqrt{\lambda_x^2-4\lambda_o^2}}{2\lambda_o^2} - 1}\;;\; \lambda_y \leq \lambda_x \quad (3)$$

have to be eliminated. It may be noted that these expressions yield λ_o for $\lambda_y \to \infty$ ($\lambda_x \to \infty$). Both curves meet at the point $\lambda_x = \lambda_y = 2\lambda_o$.

The result obtained with the modified radiation condition is displayed in Fig. 2. Obviously, a substantial improvement is attained. Tests have shown that the wave reflections emanating from the modified radiation condition are similarly weak as those caused by a Rayleigh damping layer extending over 20 model levels and a thickness of two vertical wavelengths. It is mentioned that the "nesting" of the radiation condition can be applied iteratively to more than two nesting levels. Thus, the full spectrum of vertically propagating gravity waves can be radiated upward for arbitrarily high horizontal resolutions. Moreover, an option has been implemented to switch off the local computation of the radiation condition for nests exceeding a certain nesting level. In this case, the radiation condition is interpolated from the next coarser domain without filtering. This option is appropriate for horizontal resolutions $\lesssim$ 1 km since gravity waves

shorter than $\sim$ 5..10 km (depending on atmospheric conditions) are vertically damped and thus are not treated properly with a radiation condition.

4. Suggestions for further improvements

The smoother-desmoother applied to the meteorological fields after feedback from a nest to a coarser domain causes appreciable smoothing of wavelengths between $4\Delta x$ and $6\Delta x$. Thus, the amplitude of the interpolated radiation condition is too low in the corresponding wavelength range. This may cause partial wave reflections. Probably, a further improvement of the radiation condition can be attained by enlarging the subdomain used for its computation to 19×19 grid points. Then, only wavelengths $\geq 6\Delta x$ have to be interpolated from the next coarser domain. However, a disadvantage of enlarging the subdomain is that the "bands" near each lateral boundary where computing the radiation condition is not possible enlarge, too. Thus, the current 13×13 grid should be retained near the lateral boundaries.

In addition, Coriolis and nonhydrostatic effects should be taken into account. While the presence of Coriolis force reduces the vertical wavelength of gravity waves, nonhydrostatic effects increase it substantially. This has severe implications for the phase shift between the two uppermost model levels that is computed by the radiation condition. In particular, there is no phase shift at all for vertically damped gravity waves, i.e. for horizontal wavelengths less than $2\pi\frac{U}{N}$.

References

Klemp, J. B., and D. K. Lilly, 1978: Numerical simulation of hydrostatic mountain waves. *J. Atmos. Sci.*, **35**, 78–107.

Saito, K., and M. Ikawa, 1991: A numerical study of the local downslope wind Yamaji-kaze in Japan. *J. Met. Soc. Japan*, **69**, 31–56.